Journal of Photochemistry, 4 (1975) 281 - 297

IMPRISONMENT AND ABSORPTION OF RESONANCE RADIATION

M. J. BOXALL, C. J. CHAPMAN and R. P. WAYNE
Physical Chemistry Laboratory, South Parks Road, Oxford, OX1 3QZ (Gt. Britain)
(Received March 23, 1975)

Summary

Measurements of the effective lifetimes for decay of resonance radiation in optically dense systems are described. For Ar($^3P_1 \rightarrow {}^1S_0$) emission, the lifetime increases with [Ar] up to a limiting value of ~ 9 μs at [Ar] > 2×10^{17} atom/cm^3.

The lifetime measurements are shown to be consistent with the imprisonment of radiation, and escape mainly through the wings of a pressure broadened line described by a simple Holtsmark profile. For the pulsed excitation used, the lifetime (as measured at the detector) appears to be determined by escape from the zone actually absorbing the exciting radiation. This result allows the use of similar lifetime measurements in studies of fluorescence quenching. Experimental evidence is given for the trapping of radiation (λ = 130.2 - 130.6 nm) in atomic oxygen at [O] = 10^{15} atom/cm^3, but not in atomic hydrogen at the same concentration.

The line profiles adopted were also used to predict the exciting lamp spectral output and hence the integrated absorption by Ar of both the lamp radiation and of resonance fluorescence. It is shown that both the lamp and the fluorescence are heavily reversed. For the fluorescence this shows that the detector responds mainly to radiation emanating from near the spatial centre of the fluorescence cell. This conclusion is therefore the same as the requirements for the model of radiation trapping.

Introduction

In an earlier paper [1], we described the quenching of argon resonance fluorescence at λ = 106.7 nm (from the $^3P_1$ state) in an optically dense system. It was shown that the steady state (Stern–Volmer) quenching rates could be explained on the basis of extensive radiation imprisonment of the fluorescent emission. Studies of Penning ionization [2] by Ar($^3P_1$) are also consistent with such trapping. The deliberate use of a heavily trapped system suggests itself as a general means for the study of deactivation of excited state species for which the natural radiative lifetime is short compared with the lifetime with respect to quenching. There is a limit to the concentration of quencher that can be employed before pressure broadening

of the absorption profiles invalidates the Stern–Volmer analysis [3]. Excitation homogeneous with respect to the linear distance from the source can be achieved even where the optical depth is great at the line centre by employing a highly reversed lamp [1]. A forthcoming paper [4] discusses quenching experiments with imprisoned radiation, and the results of steady state experiments are compared with those of time-resolved studies. Pulsed excitation is employed in the time-resolved experiments, and also to provide a measurement of the effective radiative lifetime to be used in the steady state calculations. The escape of imprisoned radiation from a system that has reached quasi-equilibrium can be described by a rate law which is common to all parts of the enclosure. Measurements of intensity in the presence of quencher can then be used, either directly in the time-resolved case, or in combination with the radiative lifetime for the steady state situation, to give the rate constant for quenching. However, if radiative transport of excitation has not reached its own steady state during an excitation pulse, the presence of a deactivator may lead to a changed distribution of emitters and an erroneous rate constant for quenching.

The objects of the present work are twofold. First, we wished to show that the observed lifetimes of unquenched fluorescence were consistent with sensible models of radiation trapping. Secondly, we sought to discover the extent to which radiative transfer *during* the excitation pulse might invalidate the assumptions made in quenching experiments.

Experimental

Materials

Argon, helium, oxygen and hydrogen, obtained from cylinders, were passed through phosphorus pentoxide drying tubes and, at low pressure, through liquid nitrogen traps before being admitted to the flow tube. As mentioned in an earlier paper [1], the argon used contained nitrogen at a concentration of between 0.05 and 0.1%. "X" grade argon, supplied by B.O.C., was used in the sealed resonance lamps.

Apparatus

The experiments described here were performed in a low pressure flow system similar to that described previously [1]. The cross-section of the flow tube, illustrating the arrangement of the resonance lamp, detector, filter cells and baffles, is shown in Fig. 1. The baffles and Wood's horn were incorporated in order to reduce the amount of scattered radiation reaching the detector (channel electron multiplier). Using the arrangement shown, the contribution from scattered radiation was a small fraction ($< 2\%$) of the total signal when the resonance lamp was operated in the continuous mode with a pressure of 1 Torr of argon in the flow tube.

A flow of argon was employed to prevent the build up of impurities in the illuminated region. Flow velocities were about 30 cm/s. When a pressure of less than 2 Torr of argon was required, it was necessary to perform

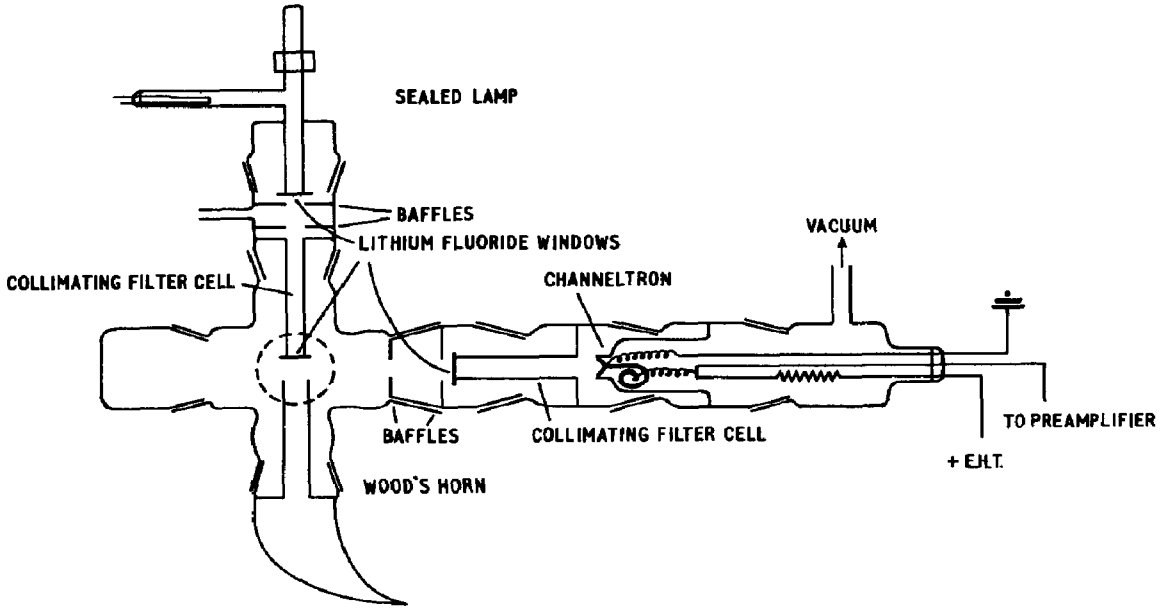

Fig. 1. Cross-section of flow tube showing arrangement of lamp, detector and collimators.

experiments in the presence of a helium buffer gas which prevented the back diffusion of pump oil vapours into the observation region.

Light source

Two types of Ar resonance lamp were used. In some experiments, a flowing lamp was used, the flow gas being dried Ar or Ar/He. For the quantitative studies, a sealed lamp containing ~ 1 Torr of Ar was employed. The lamps were in all cases energized by an electrodeless microwave discharge.

The output of the sealed lamp was checked with a McPherson model 218 (0.3 m) spectrometer, and is shown in Fig. 2. Even after firing the getter, some Lyman-α impurity radiation remained. Some emission at λ = 104.8 nm, from the Ar($^1P_1 \rightarrow {}^1S_0$) transition, was also present. The intensity of the 104.8 nm line is theoretically three times greater than that of the 106.7 nm ($^3P_1 \rightarrow {}^1S_0$) line in an unreversed source, so that the observed lower intensity at λ = 104.8 nm indicates that the $^1P_1 \rightarrow {}^1S_0$ line was strongly absorbed by the LiF window or highly reversed, or both. In the system used for the fluorescence experiments there were three lithium fluoride windows, as opposed to only one in the lamp/spectrometer combination, and consequently the Ar($^1P_1 \rightarrow {}^1S_0$) radiation was not expected to be of importance. The sources for H- and O- resonance radiation were, respectively, a static lamp containing 1% H_2 in Ar and a flowing lamp using a gas mixture of 5% O_2 in Ar.

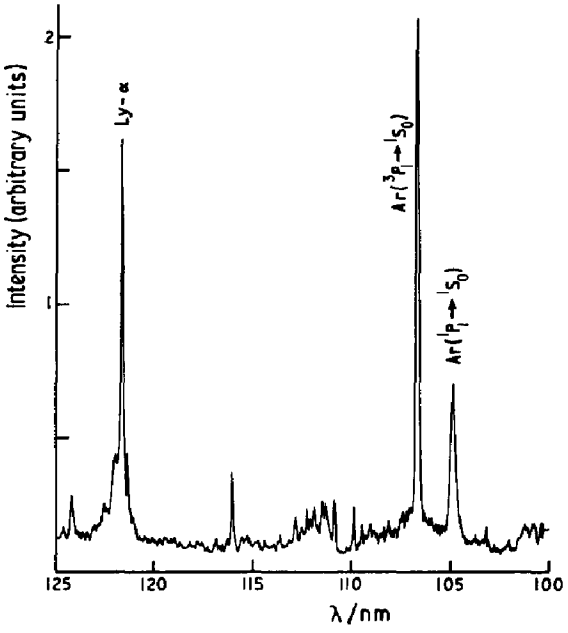

Fig. 2. Emission spectrum of the sealed argon resonance lamp.

Lifetime measurements

The extent of radiation trapping in argon was determined by monitoring the intensity of resonance fluorescence as a function of time following pulsed excitation.

Modulation of exciting radiation

To obtain a pulsed source of exciting radiation the microwave generator (Microtron 2000L) used to drive the resonance lamp, was modulated so that it produced a series of pulses of energy superimposed upon a very weak background energy level. The steady power dissipation was reduced by placing a large resistance (150 kΩ) in series with the magnetron anode. Pulses of microwaves were then produced by feeding ~ 1 μs pulses to the magnetron cathode *via* a pulse transformer at a repetition frequency of about 15 kHz. The resulting microwave output consisted of a series of bursts of radiation of about 1 μs duration with almost no subsequent ringing. The radiation produced by the pulse-excited resonance lamp had a short rise time (~ 500 ns) but a much longer decay time (~ 5 μs).

The multichannel scaler

The decay of radiation was measured using a specially constructed multichannel scaler. The scaler possessed forty channels which could be accessed sequentially at rates of up to 1 μs per channel. Each scan was triggered synchronously with the microwave pulses. The output of the multichannel scaler was displayed both digitally, and in analogue form on an oscilloscope. Figure 3 shows typical decay plots for the sealed Ar-resonance lamp and for resonance fluorescence.

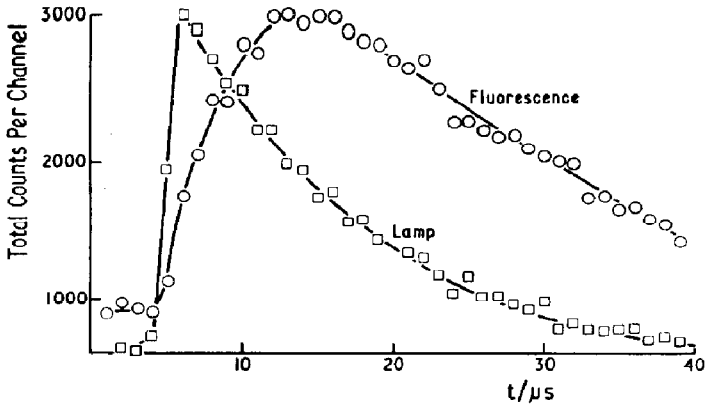

Fig. 3. Lamp (□) and fluorescence (○) decay profiles. [Ar] = 2.2×10^{17} atom/cm^3 in flow tube for fluorescence experiment; calculated fluorescence lifetime = 8.3 μs.

The time profile of exciting radiation

The different spectral lines present in the lamp output decayed at slightly different rates — the shorter the wavelength of the emission the greater the decay rate (see Table 1). The decay rate of the 106.7 nm line was equal to within about 10% of the overall decay rate. Decay rates varied according to the tuning and matching of the microwave cavity. In subsequent experiments, therefore, the decay rate of the total radiation was measured in each run, and the decay rate of the 106.7 nm radiation was assumed to be the same.

Deconvolution of excitation and fluorescence decays

Because the pulse of exciting radiation did not have a sharp cut-off it was necessary, when measuring fluorescence lifetimes, to separate the effect of the excitation pulse from the observed fluorescence decay. The true fluorescence decay rate was extracted numerically from the observed data. The profile of the excitation pulse (corrected for the low intensity unmodulated background) was convoluted with a simple exponential decay, of the form $\exp(-kt)$, to produce a theoretical curve for fluorescence decay. The theoretical curve was then compared with the observed decay curve, also corrected for background, by a χ^2 "goodness-of-fit" test. The value of the exponent k was varied to minimize χ^2. Lifetimes (*i.e.* $1/k$) so obtained were always repeatable to ± 15%.

Results and Discussion

As shown above, the predominant argon resonance line in the lamp output is that at 106.7 nm. We have previously [1] demonstrated that processes involving the metastable $^3P_2$ state of Ar must be unimportant in the excitation of fluorescence in our system, and that at [Ar] $< 5 \times 10^{17}$ atom/cm^3 the only significant steps are:

$$Ar(^1S_0) + h\nu\ (\lambda = 106.7\ \text{nm}) \rightarrow Ar(^3P_1) \quad (1)$$

$$Ar(^3P_1) \rightarrow Ar(^1S_0) + h\nu\ (\lambda = 106.7\ \text{nm}) \quad (2)$$

TABLE 1

Lifetimes of the lines present in the sealed argon resonance lamp.

Resonance line	Wavelength (nm)	Lifetimes (μs)	Mean lifetime (μs)
Ar($^1P_1 \rightarrow {}^1S_0$)	104.8	4.0 3.6 4.0	3.9
Ar($^3P_1 \rightarrow {}^1S_0$)	106.7	8.9 9.2 8.6	8.9
H (Lyman α)	121.5	11.6 11.9	11.8
Total lamp emission (central maximum)		10.1	10.1
Total lamp emission (flow tube scatter)		10.0 10.0 10.9 10.0	10.2

In this discussion, we therefore consider first the shape of the resonance line and, from the line shape, calculate the spectral output of the excitation lamp. We then determine the effective absorption cross-sections of Ar for this radiation. Finally, we show that the observed radiative lifetimes are consistent with resonance trapping as described by a simple model. The spectroscopic parameters used in the trapping model are the same as those employed in the absorption calculations.

Line shape

The shape and width of an isolated spectral line is determined largely by natural, Doppler and collision (pressure) broadening [3]. It will be shown in the next section that the source lamp is heavily reversed and that there is negligible emission near the line centre. Under these circumstances, we may use the simplified [3] expression for the absorption cross-section, $\sigma(\nu)$:

$$\sigma(\nu) = \sigma_0\{\exp(-x^2) + a/\pi^{1/2}x^2\} \tag{3}$$

Here σ_0 is the absorption cross-section at the line centre, ν_0, and x is given for an atomic mass M by:

$$x = \frac{\nu - \nu_0}{\nu_0} \cdot c \cdot \left(\frac{2RT}{M}\right)^{-1/2} \tag{4}$$

The parameter a is associated with collision and natural broadening, and it may be shown [3] that:

$$a = \frac{(A + A_p)c}{4\pi\nu_0\nu_0} \tag{5}$$

where $v_0 = (2RT/M)^{1/2}$. A is the natural Einstein A-coefficient and A_p varies directly with pressure. The validity of the formulae depends on several factors. Expression (3) requires that $x > 2$ and $a \ll 1$. We will show subsequently that these conditions are met. It is more difficult to establish whether the pressure broadening is adequately described by the dispersion equations, or the equivalent statistical form [5]. For self-broadening of a resonance transition, dipole–dipole interactions are indeed likely to be relatively important. However, at large $\Delta\nu(= \nu - \nu_0)$, the intensity may no longer fall off as $(\Delta\nu)^{-2}$; and there may be a marked asymmetry between long- and short-wave tails. This situation is known to be most important in systems where the oscillator strength, f, is appreciably less than unity (*e.g.* in Hg $^3P_1 \rightarrow {}^1S_0$, for which [6] $f = 0.03$). For Ar($^3P_1 \rightarrow {}^1S_0$), f is [7 - 9] 0.02 to 0.06. In the rest of this discussion, we have assumed that the $(\Delta\nu)^{-2}$ proportionality does, in fact, hold. We have employed a form for A_p derived from the expressions of Weiskopf (and quoted by Mitchell and Zemansky [3] as their equations 123 and 125) for Holtsmark broadening. The result is:

$$\frac{A_p}{A} \sim \frac{\lambda_0^3}{8\,(2)^{1/2}\pi}\,\frac{g_2}{g_1}\,n \qquad (6)$$

where g_2 and g_1 are the degeneracies of upper and lower states respectively, and n is the concentration of atoms.

Light sources

The lamp consists of a microwave discharge, followed by approximately a 10 cm path of Ar at the lamp pressure. This resonant absorber is optically thick near the centre of the emission line. Kaufman and Parkes [10] have pointed out that in these circumstances, trapping of resonance radiation can lead to a near-uniform concentration distribution of emitters. Whether the lamp behaves (i) as a simple uniform-distribution source or (ii) as a two-layer emitter–absorber combination (the two extremes) depends in part on the optical depth of the lamp and in part on geometrical factors such as the ratio of length to diameter of the lamp tube. For argon concentrations such that radiation is very highly trapped (*i.e.* the medium is optically extremely dense), and for a long thin absorbing layer in front of the plasma (radius 0.5 cm, length 10 cm), a real lamp is likely to approximate more closely to model (ii) than to model (i). We shall explore further the question of emission of trapped resonance fluorescence in a later section. For the time being, it is worth noting that the experimentally determined absorption cross-sections of argon for the lamp radiation (next section) are four or more orders of magnitude smaller than the expected cross-section at the line centre. This result suggests highly reversed radiation from the source, a situation predicted by model (ii) but not by model (i).

The output of the two-layer lamp may be calculated in the manner described by Braun and Carrington [11]. It is assumed that the frequency dependence of the initial emission from the plasma follows $\sigma(\nu)$, so that $I(\nu)$ at the LiF window is given by:

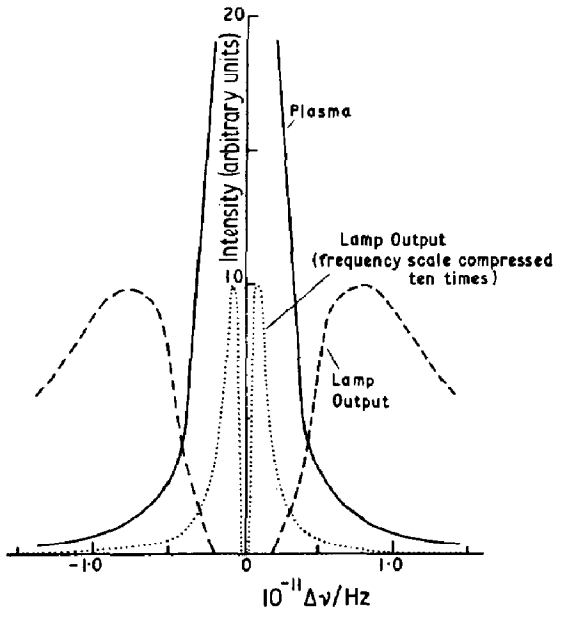

Fig. 4. Calculated spectral profiles of plasma and lamp output in the two-layer lamp. Plasma temperature = 600 K; absorber temperature = 300 K, path = 10 cm. [Ar] = 3.5 × 10^{16} atom/cm^3.

$$I^{\text{lamp}}(\nu) = I_s \sigma_s(\nu) \exp(-\sigma_l(\nu) n_l l_l) \tag{8}$$

I_s is the constant of proportionality, and n_l, l_l are the concentration of Ar and the optical path in the lamp; subscripts s refer to the plasma source. Figure 4 shows the results of typical calculations with the effective temperature of the plasma taken to be 600 K (this turns out to be unimportant: see next section) and with σ_0 given by [3]:

$$\sigma_0 = \frac{\lambda_0^3}{8\pi} \cdot \frac{g_2}{g_1} \frac{A}{\pi^{1/2} v_0} \tag{9}$$

A is taken [9] to be 1.2×10^8 s^{-1}, although very similar results are obtained with 4.7×10^7 s^{-1} given by Morack and Fairchild [8].

Calculations show that at no lamp pressure used (> 0.1 Torr) was there any significant emission at $\Delta\nu < 10^{10}$ Hz. This value of $\Delta\nu$ corresponds to $x \sim 5$. Thus the requirement $x > 2$ for application of the approximation (3) was always satisfied. For the highest pressures used (generally $n \gg 5 \times 10^{17}$ atom/cm^3; $a < 0.4$;) the approximation could, in principle, become inexact. However, the calculated lamp output will remain unaffected because of the vanishingly small contribution to the spectral distribution near the line centre.

Absorption

The transmission of the resonance lamp emission through argon contained in a filter cell can now be calculated at each frequency:

$$I^{\text{trans}}(\nu) = I^{\text{lamp}}(\nu) \exp(-\sigma(\nu) n_a l_a) \tag{10}$$

where n_a and l_a are the concentration and path of the absorber.

Kaufman and Parkes [10] have used a diffusion model of radiation trapping to analyze the errors introduced by fluorescent scattering into resonance absorption measurements. We shall compare our calculations with the results obtained using either resonance fluorescence or Penning ionization as "specific" detectors of Ar-resonance radiation and given in ref. [1]. Figure 1 of that paper shows that the absorbing argon (which acts as detector) was ~ 3 cm beyond the end of the absorption tube, which was itself 10 cm long and 0.5 cm radius. The discussion of Kaufman and Parkes [10] (eqns. (22) or (23): the latter is inexact for our length to radius ratio) makes it clear that, with our experimental arrangements, scattered radiation does not significantly contribute to the detected signal.

Use of a detector which itself has the spectral absorption characteristics of argon requires that the values of $I^{\text{trans}}(\nu)$ be suitably weighted. Further, the light emerging from the filter cell passes through another absorbing layer (of 3.0 cm thickness in our experiments). Thus we define an overall optical density, δ, given by the relation:

$$\delta = -\log_{10} \frac{\int_{-\infty}^{\infty} I^{\text{trans}}(\nu) \exp(-\sigma_d(\nu) n_d \times 3.0)[1 - \exp(-\sigma_d(\nu) n_d \times 1.0)]}{\int_{-\infty}^{\infty} I^{\text{lamp}}(\nu) \exp(-\sigma_d(\nu) n_d \times 3.0)[1 - \exp(-\sigma_d(\nu) n_d \times 1.0)]} \tag{11}$$

where $\sigma_d(\nu)$ and n_d refer to the absorption cross-section and argon concentration in the flow tube "detector". The integrations were performed numerically, using the form of eqn. (3) for $\sigma(\nu)$, between limits chosen to include 99% of the lamp output.

It is not to be expected [11] that δ will be a strictly linear function of n, although over a limited concentration range it may approximate to one, as we previously observed [1]. Figure 5 shows δ calculated as a function of n_a; the parameters are specified in the legend. Experimental results from our earlier work are also displayed for comparison. The good agreement suggests both that the two-layer lamp model adequately represents the physical situation, and that the line profiles used are reasonable. Effective absorption cross-sections, σ_a, are calculated from a forced linear fit of δ to [Ar], from [Ar] = 0 to 3.0×10^{17} atom/cm^3. Table 2 compares experiment and calculation.

Two interesting features emerge from the calculations. First, there is virtually no dependence of δ on the value chosen for the plasma temperature, since little of the lamp output is spectrally determined by Doppler broadening. Secondly, anomalous values of a (or A_p) for the plasma do not affect δ. This somewhat unexpected result arises from the form of eqn. (3);

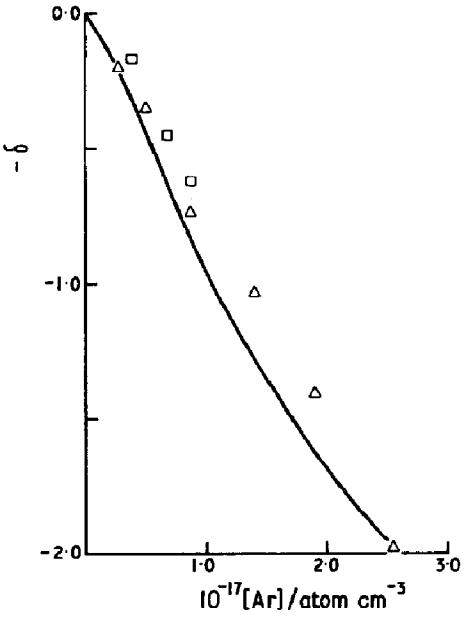

Fig. 5. Calculated and observed average optical densities for absorption of reversed radiation. Experimental points from ref. [1]: Δ, resonance fluorescence; □, Penning ionization, as "detector". Solid curve calculated for plasma temperature = 600 K, all other temperatures 300 K. [Ar] = 4.0×10^{16} atom/cm^3 in the lamp; [Ar] = 5.0×10^{16} atom/cm^3 in the "detector". Path lengths of Ar in both lamp and filter = 10.0 cm.

TABLE 2

Apparent absorption cross-sections using resonance fluorescence as indicator

[Ar] in flow tube $\times 10^{-16}$ (atom/cm^3)	$\sigma_a \times 10^{18}$ (cm^2)	
	Experimental [1]	Calculated
1.3	1.5 ± 0.1	1.8
5.0	1.5 ± 0.1	1.7
15.0	1.3 ± 0.1	1.2

the radiation leaving the lamp is described almost entirely by the $(a/\pi^{1/3}x^2)$ term so that a can then factorize out of the intensity terms in the integrals of eqn. (11).

The attenuation of resonance fluorescence, excited in the flow tube, should indicate whether the escaping fluorescent emission is better described as radiation from a homogeneously excited gas or from a two-layer emitter–absorber system. The temperature and pressure of the primary source are well-defined, and there is no problem about anomalous collision broadening resulting from the presence of an electric discharge. The experimental cross-sections [1] are all less than 2×10^{-18} cm^2, suggesting that, as in the lamps, a "reversing" mechanism must operate. Figure 6 compares the experiments

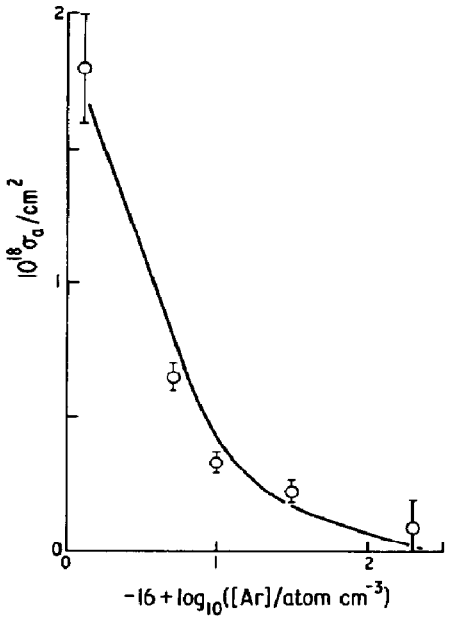

Fig. 6. Observed [1] (points) and calculated (curve) average cross-sections for absorption of argon resonance radiation as a function of [Ar] in the flow tube.

(points) with the values of $\sigma_a (= \delta / n_a l_a$, at $n_a = 1.0 \times 10^{17}$ atom/cm^3) calculated (solid curve) using a two layer model. The good agreement indicates that the two-layer model mimics the optical conditions in the flow tube.

A decrease in the path of argon allowed for absorption in the flow tube leads to predicted values of σ_a larger than those observed.

These results suggest that, even though the emission may be fairly homogeneous as a result of radiation trapping, the detector has a directional response towards radiation from the centre of the flow tube considerably greater than that for radiation from the periphery. The detector is quite well collimated in these experiments, since it sits at the back of the 10 cm filter cell. Thus, although the ratio of length to radius is not so favourable [10] compared with the lamp-filtering experiments, the contribution from scattered (trapped) radiation is still attenuated sharply with distance from the irradiated zone. This conclusion is of some relevance with regard to the discussion of radiative lifetimes given in the next section.

Radiation trapping

At concentrations for which the optical depth is small even near the line centre, resonance radiation may escape in a single emission step. However, at higher concentrations, the excitation may migrate from atom to atom until emission occurs at a frequency or geometrical position for which the optical depth is small. The radiation is then said to be "trapped" or "imprisoned" and the effective radiative lifetime will greatly exceed the true radiative lifetime. The frequency distribution of the primary exciting

radiation is converted in the course of a few steps to a frequency distribution (locally, before re-absorption) appropriate to the physical conditions of the emitting gas†.

Compton [13] and Milne [14] treated the escape of imprisoned radiation in terms of diffusion, although Holstein [15] subsequently showed that the diffusion theories were unacceptable because of the impossibility of defining a mean free path for the photons. Holstein's method [15, 16] consists of formulating an integro-differential equation for the probability that a photon emitted at one point is absorbed in a volume element at another point. His solutions are analytic approximations for cases of large optical depth, although the same treatment has been used (*e.g.* ref. 17) to provide exact numerical solutions for intermediate optical depths. Several other treatments of radiation trapping have been given (see, for example, ref. 18 and its introduction), but in this section we apply the results of Holstein and of Walsh [19]. The probability, $T(\rho)$, that a photon will be transmitted a distance ρ is first calculated for different forms of line shape. Then the transfer and escape of photons is examined for enclosures of different geometries (*e.g.* infinite slabs or cylinders). Solutions of the transfer equations show that there are several escape modes, i, which satisfy the equations

$$n^*(r,t) = n^*(r,0)\exp(-\beta_i t) \tag{12}$$

At "long" times, escape is *via* the lowest decay mode, characterized by β_1. n^* represents the concentration of excited species at any point r. The spatial distribution is determined by the transfer and escape processes, but the concentration at all points is governed temporally by common values of β_i. It may be shown [19] that β_1 is approximately related to $T(\rho)$ by the equation:

$$\beta_1 = \frac{T(\rho)}{\kappa} A \tag{13}$$

The constant κ then depends on the geometry of the system and the form of line broadening [16, 19]. Walsh [19] gives the following forms for κ and $T(\rho)$ in an infinite cylinder:

$$T_d(\rho) = \frac{1}{k_0\rho(\pi \ln k_0\rho)}; \qquad \kappa_d = 1.60 \tag{14a}$$

$$T_c(\rho) = \frac{1}{\pi^{1/2}}\left(\frac{\pi^{1/2}a}{k_0\rho}\right)^{1/2}; \qquad \kappa_c = 1.115 \tag{14b}$$

$$T_{cd}(\rho) = \frac{2a}{\pi(\ln k_0\rho)}; \qquad \kappa_{cd} = 1.00 \tag{14c}$$

†It has recently been pointed out [12] in connection with a study of the trapping of 104.8 nm, $^1P_1 \rightarrow {}^1S_0$, radiation in Ar, that redistribution of absorbed and emitted frequencies may not always occur at low pressures (< 0.5 Torr). However, the radiative lifetime of the $^1P_1 \rightarrow {}^1S_0$ transition is five times less than that for the $^3P_1 \rightarrow {}^1S_0$ transition, so we expect redistribution to be effectively complete.

In these equations, $k_0 = \sigma_0 n$, and the subscripts d, c, and cd refer to Doppler broadening, collision broadening (pure dispersion or dipole–dipole interaction; natural broadening may be included), and emission from collision-broadened wings with Doppler-type absorption. For a real system, the $T(\rho)$ conditions may be combined [19] to give:

$$T(\rho) = T_d(\rho)\exp[-\pi T_{cd}^2(\rho)/4T_c^2(\rho)] + T_c E_2\{\pi^{1/2} T_{cd}(\rho)/2T_c(\rho)\} \qquad (15)$$

where E_2 is the error integral of the function within parenthesis.

The application of eqns. (13) - (15) to our experiments needs some consideration. Since the strongly reversed exciting radiation is fairly weakly absorbed (see above), and collimated, the energy input is into a cylinder of radius ~ 0.5 cm. This is not an infinite cylinder, nor are the bounds of the enclosure cylindrical. However, κ does not seem to depart grossly from unity for other geometries so that, for the order-of-magnitude calculations presented here, we retain the values of κ given in eqns. (14). A more serious problem concerns the distribution of excitation. With a lamp pulse of duration very short compared to $1/\beta_1$, the excitation will reside initially almost entirely in the illuminated cylinder, from which it will be radiatively transported. The measured lifetime will then depend on the decay of intensity from that part of the system viewed by the detector. Deconvolution of lamp and fluorescence lifetimes involves imposition of an exponential decay function on the lamp intensity–time profile (see experimental section), and since the rise time of the lamp is short compared with the trapping times given later, it will be taken that the pumping and escape functions, though not the concentration of excited atoms, are at any time independent of preceding events. It may be noted that the lamp is off between pulses for sufficiently long to ensure essentially complete decay of excitation. We are thus making the reasonable assumption that back-transport of radiation from outer layers does not greatly affect n^* in the central (high concentration) zone. This view appears to be borne out by the Stern–Volmer quenching constants measured using continuous and pulsed excitation [4]. The similarity of the constants suggests that β_1 is nearly the same regardless of whether the radiation in the enclosure has or has not come to a steady state†. In any case, it follows from the values of κ that transport over the distance ρ largely governs escape. We therefore use values of β_1 calculated from eqns. (13) - (15) while recognizing that they apply to a somewhat different situation.

Two extreme cases may now be considered as first approximations to calculate the effective radiative lifetime as determined by intensity measurements at the detector. In these approximations, we also assume that observed light originates mainly from the central irradiated zone, in accordance with the evidence of the absorption experiments. The radiation is thus

---

†The statement is true so long as higher modes of escape with $\beta_i \gg \beta_1$ do not make an important contribution: most of the observed radiation *must* be characterized by β_1 in order that fluorescence quenching rates [1, 4] do not exceed gas kinetics.

considered to be trapped in a cylinder of radius r_1 ($\simeq 0.5$ cm) and to escape from it. The two cases are: (i) the *radiation* is assumed to be in its steady state, homogeneous, distribution within the cylinder, but zero outside it. Escape rates are determined directly by eqns. (13) and (15) with $\rho = r_1$; and (ii) the *concentrations* are assumed initially to be homogeneous as a result of even illumination. The escape rate in cylindrical mode is now calculated from a cylindrical element of radius r and thickness dr. An average value of $\overline{\beta}$ is obtained in the following way. The intensity at the detector is summed numerically over the elements, due weight being given to the change of emitting volume with radius, and the variation of total intensity with time calculated. The time dependence of intensity is surprisingly close to being exponential, so that an average $\overline{\beta}$ may be extracted.

The expression given by Walsh [19] to combine eqns. (14), *viz*:

$$\beta_1 = \beta_{1d}\exp(-\beta_{1cd}^2/\beta_{1c}^2) + \beta_{1c}E_2(\beta_{1cd}/\beta_c) \qquad (16)$$

was used to evaluate β_1 for $r_1 = 0.5$ cm, and to obtain an average $\overline{\beta}$ as described in (ii). Figure 7 shows the calculated lifetimes ($1/\beta$), together with the experimentally measured values. The calculations use $A = 1.2 \times 10^8$ s^{-1} [6]; a smaller value, suggested by the work of Morack and Fairchild [8], leads to greater predicted lifetimes.

The lifetimes calculated for model (ii), which is regarded as more realistic than model (i), are in quite good agreement with the observations at high [Ar]. At high pressures, radiation escape is almost entirely confined to the pressure-broadened wings of the line. The predicted lifetimes appear to rise more sharply with [Ar] than the observed ones. This tendency could be corrected by employing a value of A_p smaller† than that implied by eqn. (6), but the calculated limiting high pressure lifetime would then be considerably too large. The results of calculation and experiment could be reconciled if broadening were a consequence of a combination of weak dipole–dipole interaction (giving a slow rise of lifetime with concentration) and a van der Waals interaction (which actually predicts a *decrease* in lifetime with increased pressure [16]).

Whatever the exact mechanism is for pressure broadening, it is clear that the trapping cannot be effective over a distance much greater than the 0.5 cm radius used in our calculations without the expected lifetimes greatly exceeding those measured. A recently developed numerical model [20] of radiation trapping in a system of our geometry shows that about 90% of the emitted radiation is indeed expected to come from the central, illuminated, core of the system. Thus the most important conclusion of the present experiments is that lifetimes do indeed appear to be determined by radiation imprisonment, but that this imprisonment is largely confined (so far as the detector is concerned) to the central region of the flow tube, which, on the evidence of the absorption experiments, is in any case the major contributor

†The equation certainly overestimates the observed broadening of the Na D lines by a factor of between 2 and 10 (see ref. [3], pp. 186 - 187).

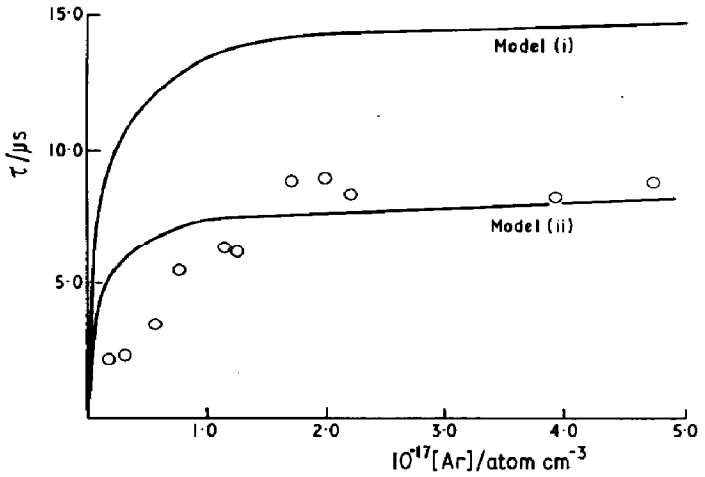

Fig. 7. Measured radiative lifetimes (points) as a function of [Ar] in the flow tube; excitation by sealed lamp. The solid curves show lifetimes calculated on the basis of the two models discussed in the text.

to the detected radiation. This conclusion means that fluorescence quenching experiments are not invalidated as a result of changes in spatial distribution of emitters in the presence of quencher.

A number of experiments were performed to examine the effect of varying the pressure of argon in the exciting source; flowing lamps were used for this purpose. Frequency redistribution, as discussed in the first paragraph of this section, should make the probability of trapping independent of the exciting line profile. However, with a strongly absorbed source, the mean distance over which radiation is imprisoned will be greater than with a weakly absorbed source. To accentuate the distance effect, the experiments were carried out with the lamp set back by 3 cm from the part of the flow tube viewed by the detector. Figure 8 shows results for lamp pressures of 0.5 and 4.0 Torr. The measured lifetimes are longer, and rise more rapidly, for the lower pressure (less reversed) lamp, as anticipated. The lifetimes at high [Ar] in the flow tube ($\sim 4.5 \times 10^{17}$ atom/cm^3) were 14.0, 12.2, 11.0 and 10.3 μs respectively for excitation by lamps containing 0.02, 0.5, 4.0 and 8.5 Torr of argon.

The lifetimes measured in this work are consistent with other measurements made with imprisoned radiation in rare gases. Using pulsed electron excitation, Thonnard and Hurst [21] observed lifetimes of 7.7 μs and 3.2 μs for Ar($^3P_1$) and Ar($^1P_1$) in 25 Torr ($\sim 8 \times 10^{17}$ atom/cm^3) of Ar in a rather different optical system. The value of 7.7 μs can be compared with our lifetime of 8.7 μs for Ar($^3P_1$) at [Ar] = 5×10^{17} atom/cm^3. Payne *et al.* [12] report a limiting lifetime of 2.5 - 3.3 μs for the $^1P_1$ state in a 2.2 cm diameter cylinder. In neon, the corresponding trapped lifetimes are [22] $\sim$ 5.0 μs and $\sim$ 84 μs, for the $^1P_1$ and $^3P_1$ states. Table 3 expresses these results as ratios of trapped to natural lifetimes. These ratios are all similar, lying within a factor of 3 of each other.

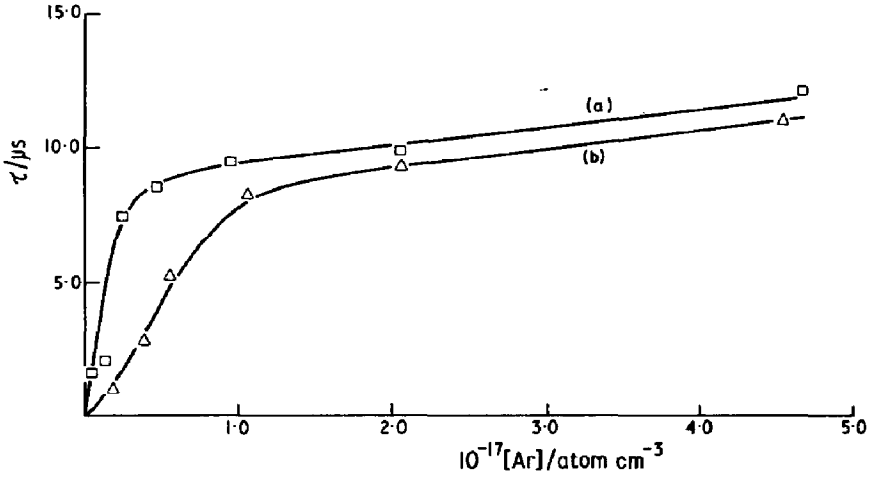

Fig. 8. Radiative lifetimes measured using flowing lamps for excitation: (a), □, p_{Ar} = 0.5 Torr in lamp; (b), △, p_{Ar} = 4.0 Torr in lamp.

TABLE 3

Ratio of trapped lifetime at high pressure to natural radiative lifetime

State	Ratio of lifetimes	Reference
$Ar(^3P_1)$	1.05×10^3	this work
$Ar(^3P_1)$	0.92×10^3	21
$Ne(^3P_1)$	2.65×10^3	22
$Ar(^1P_1)$	$\sim 1.5 \times 10^3$	12
$Ar(^1P_1)$	1.6×10^3	21
$Ne(^1P_1)$	2.67×10^3	22

We have made some preliminary attempts to observe trapping of resonance radiation in atomic hydrogen and atomic oxygen, at atom concentrations up to 10^{15} cm^{-3}. No trapping was observed in H, but a radiative lifetime of 0.8 μs was determined in O. This value is subject to considerable error, since it is only comparable with the time resolution of the system (1 μs per channel), but suggests appreciable trapping since the A factors for the O resonance triplet (1302, 1305, 1306 Å) are 2.1, 1.3, 0.4×10^8 s^{-1} respectively [23].

Trapping is thus occurring in O at concentrations well below those expected in Ar. This probably results mainly from the much larger σ_0 for O compared to Ar [direct measurements [7] give 32.7×10^{-13} cm^2 for the sum of the three O lines against 0.86×10^{-13} cm^2 for $Ar(^3P_1 \rightarrow {}^1S_0)$]. For the low values of [O], collision broadening will be largely effected by the carrier gas (Ar) and thus small compared to the natural (and Doppler) broadening since there can be no dipole–dipole interaction. Escape of imprisoned radiation will then probably be determined by the Doppler shape, and increased σ_0 will greatly decrease $T(\rho)$, as expressed in eqn. (14a). Even if natural or collisional broadening play a part in radiation escape, $T(\rho)$ will

still show a reduction with increased σ_0, although to a lesser extent (eqn. 14b). For atomic hydrogen [23], $g_2/g_1 = 1$ and $A = 4.7 \times 10^8$ s^{-1}; substitution in eqn. (9) gives $\sigma_0^H/\sigma_0^{Ar} \sim 0.30$, so that trapping in H will be *less* strong than in Ar at the same concentration.

Acknowledgements

C. J. C. wishes to thank Christ Church, Oxford, for a Senior Scholarship, during the tenure of which this research was carried out. M. J. B. wishes to thank the London Borough of Merton for a maintenance award.

References

1 C. J. Chapman, A. J. Masson and R. P. Wayne, Mol. Phys., 23 (1972) 979.
2 I. D. Clark, A. J. Masson and R. P. Wayne, Mol. Phys., 23 (1972) 995.
3 A. C. G. Mitchell and M. W. Zemansky, Resonance Radiation and Excited Atoms, Cambridge University Press, London, 1934.
4 M. J. Boxall, C. J. Chapman and R. P. Wayne, J. Photochem., in preparation.
5 H. G. Kuhn, Atomic Spectra, Longmans, London, 1962.
6 H. G. Kuhn, Proc. Roy. Soc., A158 (1937) 230.
7 K. H. Becker, W. Groth and W. Jud, Z. Naturforsch., 24a (1969) 1953.
8 J. L. Morack and C. E. Fairchild, Phys. Rev., 163 (1967) 125.
9 G. M. Lawrence, Phys. Rev., 175 (1968) 40.
10 F. Kaufman and D. A. Parkes, Trans. Faraday Soc., 66 (1970) 1579.
11 W. Braun and T. Carrington, J. Quant. Spectros. Radiat. Transfer, 9 (1969) 1133.
12 M. G. Payne, J. E. Talmage, G. S. Hurst and E. B. Wagner, Phys. Rev., A9 (1974) 1050.
13 K. T. Compton, Phys. Rev., 20 (1922) 283; Phil. Mag., 45 (1923) 752.
14 E. A. Milne, J. London Math. Soc., 1 (1926) 1.
15 T. Holstein, Phys. Rev., 72 (1947) 1212.
16 T. Holstein, Phys. Rev., 83 (1951) 1159.
17 G. van Volkenburgh and T. Carrington, J. Quant. Spectros. Radiat. Transfer, 11 (1971) 1181.
18 J. J. Healy, T. F. Morse and J. W. Cipolla, Jr., J. Quant. Spectros. Radiat. Transfer, 13 (1973) 1219.
19 P. J. Walsh, Phys. Rev., 116 (1959) 511.
20 L. F. Phillips, in preparation.
21 N. Thonnard and G. S. Hurst, Phys. Rev., A5 (1972) 1110.
22 P. K. Leichner, Phys. Rev., A8 (1973) 815.
23 W. L. Weise, M. W. Smith and B. M. Miles, Atomic Transition Probabilities I, NSRDS-NBS-4 (1966).